First-principles calculation of the EPR *g* tensor in extended periodic systems

R. Declerck, V. Van Speybroeck, and M. Waroquier*
Center for Molecular Modeling, Laboratory of Theoretical Physics, Ghent University, Proeftuinstraat 86, B-9000 Gent, Belgium
(Received 12 December 2005; revised manuscript received 13 February 2006; published 20 March 2006)

A method for the *ab initio* prediction of the EPR *g* tensor for paramagnetic defects in systems under periodic boundary conditions is presented. It is based on density functional theory and the pseudopotential approximation. The formalism is applicable to crystalline and amorphous insulators, as well as to isolated molecules using a supercell technique. The method is validated by comparison with a well-established theoretical approach and experimental data for a series of small isolated molecules. Finally the EPR parameters of an O_3^- defect in a KCl lattice are evaluated following the new procedure, yielding results in good agreement with experiment and at an attractive computational cost.

DOI: 10.1103/PhysRevB.73.115113 PACS number(s): 71.15.−m, 76.30.−v, 61.72.Bb

I. INTRODUCTION

Electron paramagnetic resonance (EPR) is one of the most powerful spectroscopic techniques to identify paramagnetic defects. The *ab initio* quantum mechanical prediction of EPR quantities within density functional theory[1,2] has become possible through the pioneering work by Schreckenbach and Ziegler.[3] Since then, many other DFT-based approaches have been published. A recent overview is given in Ref. 4. These approaches are applicable to isolated systems only. Many useful applications of the EPR technique, however, involve paramagnetic defects embedded in crystals.

Recently, Pickard and Mauri[5] presented an all-electron implementation of the EPR *g* tensor applicable on extended periodic systems, using their gauge including projector augmented wave (GIPAW) method,[6] which is based on an extension to the projector augmented wave (PAW) method of Blöchl[7] and the method of Mauri *et al.*[8] (MPL). Although the original MPL method neglects the complications inherent within the pseudopotential approximation, it was found to successfully predict the nuclear magnetic resonance (NMR) properties in extended systems for elements up to Ne. The GIPAW method corrects for the deficiencies of the pseudopotentials, and in that sense one could consider it as an all-electron approach. In Ref. 6, the GIPAW method was successfully used for the calculation of all-electron NMR properties.

Almost simultaneously Sebastiani and Parrinello[9] presented a conceptually different approach for the calculation of NMR properties in extended periodic systems (hereafter referred to as the Sebastiani method). The Sebastiani method also lacks corrections for the use of pseudopotentials, and therefore can be best compared with the MPL method. In the prediction of NMR properties, its use is thus also limited to elements up to Ne.

In this paper, we propose an alternative pseudopotential approach for the calculation of the EPR *g* tensor in extended periodic systems which relies on this Sebastiani method. It was already suggested by Schreckenbach in Ref. 10 that the pseudopotential approximation could also be used for the evaluation of the *g* tensor, since the *g* tensor does not depend as crucially on the region near the core as is the case for the NMR shielding tensor. In that region, the pseudopotential approximation does not correctly describe the nodal structure of the electronic wave functions. However, no implementation was available yet that would validate or disprove this assertion. By comparison with experimental data from the literature and calculated results from Schreckenbach and Ziegler, we will investigate for which elements and at what computational cost our pseudopotential-based approach is applicable. Finally, as a typical example of a system under periodic boundary conditions, the proposed method is applied to an ozonide paramagnetic defect (O_3^-) embedded in an alkali halide lattice (KCl).

II. THEORY

The energy levels and intensities derived from EPR experiments can be reproduced using an effective Hamiltonian, expressed in terms of effective spin operators **S** (electronic) and $\mathbf{I}_n$ (nuclear). This effective Hamiltonian generally consists of three contributions,

$$H_{\text{eff}} = \sum_n \mathbf{S} \cdot \mathbf{A_n} \cdot \mathbf{I_n} + \frac{\alpha}{2} \mathbf{B} \cdot \mathbf{g} \cdot \mathbf{S} + \mathbf{S} \cdot \mathbf{D} \cdot \mathbf{S}. \qquad (1)$$

Here, $\mathbf{A_n}$ is the hyperfine tensor of rank 2 describing the coupling between the electronic **S** and the nuclear **I** spin at the center of a nucleus *n*. **g** is the *g* tensor, which describes the coupling between the electronic spin system and a constant external magnetic field **B**. **D** is the zero-field splitting tensor arising from the magnetic dipolar interactions between multiple unpaired electrons in the system. α represents the fine-structure constant and the summation *n* runs over the nuclei. Atomic units are used throughout this paper. We will consider only systems with net electronic spin 1/2 in the following, although the method can be expanded to higher spin radicals.[11]

The *g* tensor from EPR spectroscopy is a second-order property and can therefore be evaluated using double perturbation theory. The perturbation parameters are components along the axes of a given coordinate system of a constant external magnetic field, B_x, and the net electronic spin component, S_y,

 ©2006 The American Physical Society

$$g_{xy} = \frac{2}{\alpha} \left. \frac{\partial^2 \langle \Psi | H_{\text{eff}} | \Psi \rangle}{\partial B_x \partial S_y} \right|_{\boldsymbol{B}=\boldsymbol{S}=\boldsymbol{0}}. \tag{2}$$

Using the Helmann-Feynman theorem of double perturbation theory, which states that molecular orbitals have to be calculated up to first order in one parameter alone, it is sufficient to calculate the magnetic-field perturbed electronic wave function and to consider only perturbing Hamiltonians containing spin operators. In order to obtain a prediction for the g tensor from first principles, we need to equate the expectation value expression of the effective Hamiltonian with the one of a true quantum mechanical (QM) Hamiltonian in the presence of a constant external magnetic field $\mathbf{B}$,[12]

$$g_{xy} = \frac{2}{\alpha} \frac{\partial}{\partial B_x} \langle \Psi_{B_x} | \left. \frac{\partial H_{\text{QM}}}{\partial S_y} \right|_{S=0} | \Psi_{B_x} \rangle |_{\boldsymbol{B}=\boldsymbol{0}}. \tag{3}$$

Within the formalism of spin polarized density functional theory, the following expression for the components of the g tensor results:[3,5,12]

$$g_{xy} = g_e \delta_{xy} + \Delta g_{xy}^{\text{ZKE}} + \Delta g_{xy}^{\text{SO}} + \Delta g_{xy}^{\text{SOO}}, \tag{4}$$

where g_e denotes the free electron g value, and

$$\Delta g_{xy}^{\text{ZKE}} = -\alpha^2 g_e (T^\alpha - T^\beta) \delta_{xy} \tag{5}$$

is the electron Zeeman kinetic energy (ZKE) correction, which is a purely kinematic relativistic correction.

A treatment for the spin-orbit (SO) contribution was elaborated by Schreckenbach and Ziegler,[3] and is used in several other implementations,[5,13,14]

$$\Delta g_{xy}^{\text{SO}} = \alpha (g_e - 1) \int d\boldsymbol{r} [\boldsymbol{j}_{\boldsymbol{B}_x}^\alpha(\boldsymbol{r}) \times \nabla V_{\text{eff}}^\alpha(\boldsymbol{r}) - \boldsymbol{j}_{\boldsymbol{B}_x}^\beta(\boldsymbol{r}) \times \nabla V_{\text{eff}}^\beta(\boldsymbol{r})]_y. \tag{6}$$

The spin-other-orbit (SOO) correction describes the screening of the external field $\mathbf{B}$ by the induced electronic currents, as experienced by the unpaired electron. An ingenious approximate treatment for the SOO contribution, which is often found to be negligible, was suggested by Pickard and Mauri,[5]

$$\Delta g_{xy}^{\text{SOO}} = 2 \int d\boldsymbol{r} B_{y,\boldsymbol{B}_x}(\boldsymbol{r}) [\rho^\alpha(\boldsymbol{r}) - \rho^\beta(\boldsymbol{r})]. \tag{7}$$

In Eqs. (5)–(7), the superscript α denotes the spin-up channel and T^α and ρ^α are the unperturbed kinetic energy and electron probability density of the spin α channel, respectively. $\boldsymbol{j}_{B_x}^\alpha(\boldsymbol{r})$ is the electronic current density of spin α electrons, arising from a unit magnetic field coinciding with the x axis. $V_{\text{eff}}^\alpha(\boldsymbol{r})$ is an effective potential for the spin α channel, defined as

$$V_{\text{eff}}^\alpha = \sum_n \frac{-Z_{\text{ion},n}}{|\boldsymbol{r} - \boldsymbol{R}_n|} \text{erf}\left(\frac{|\boldsymbol{r} - \boldsymbol{R}_n|}{r_{c,n}} \right) + V_H + V_{\text{XC}}^\alpha, \tag{8}$$

where erf denotes the error function, Z_{ion} the ionic charge (i.e., charge of the nucleus minus charge of the core electrons), V_H the Hartree potential, and V_{XC} the exchange correlation potential. r_c gives the range of the Gaussian ionic charge distribution leading to the erf potential.[15] Similar definitions apply to the spin-down channel, denoted with β. Finally, $B_{y,B_x}(\boldsymbol{r})$ is the y component of the magnetic field due to the total induced current $\boldsymbol{j}_{B_x}^\alpha(\boldsymbol{r}) + \boldsymbol{j}_{B_x}^\beta(\boldsymbol{r})$, corrected for self-interaction by removing the contribution from the current of the unpaired electron, $\boldsymbol{j}_{B_x}^\alpha(\boldsymbol{r}) - \boldsymbol{j}_{B_x}^\beta(\boldsymbol{r})$.

A. Evaluation of $\Delta g_{xy}^{\text{ZKE}}$

In a spin-polarized DFT run, one obtains expressions for the KS orbitals and for the effective potential in both spin channels. This easily allows us to evaluate Eq. (5).

B. Evaluation of $\Delta g_{xy}^{\text{SO}}$ and $\Delta g_{xy}^{\text{SOO}}$

In order to evaluate the more elaborate terms of Eqs. (6) and (7), we need to compute the spin-dependent current densities $\boldsymbol{j}_{B_x}^\tau(\boldsymbol{r})$ ($\tau = \alpha, \beta$), and therefore we make use of the techniques proposed by Sebastiani and Parrinello[9] to include these spin-dependent current densities.

The main obstacle to evaluate these current densities is the fact that the magnetic field perturbation Hamiltonian contains the position operator. In a periodic system, this operator is not properly defined. To deal with this problem, the Sebastiani method makes use of maximally localized Wannier (MLW) orbitals,[16] which are obtained from the canonical KS orbitals by means of a unitary transformation in the subspace of occupied states,

$$|\phi_k^{(0)}\rangle = \sum_l U_{kl} |\phi_l^{\text{KS}}\rangle. \tag{9}$$

For an insulator it can be proven that these MLW orbitals decay exponentially,[17] a crucial feature in the approach. Within the continuous set of gauge transformations (CSGT) method,[18] the electronic current density can be written as a sum of three contributions,

$$\boldsymbol{j}^\tau(\boldsymbol{r}') = \sum_k^{n_\tau} \langle \phi_k^{(0)} | \boldsymbol{j}_{\boldsymbol{r}'} [|\phi_k^{(1a)}\rangle - |\phi_k^{(1b)}\rangle + |\phi_k^{(1c)}\rangle], \tag{10}$$

with the current density operator $\boldsymbol{j}_{\boldsymbol{r}'}$, $\tau = \alpha, \beta$, and

$$|\phi_k^{(1a)}\rangle = \sum_l G_{kl}(\boldsymbol{r} - \boldsymbol{d}_l) \times \boldsymbol{p} |\phi_l^{(0)}\rangle \cdot \boldsymbol{B}, \tag{11}$$

$$|\phi_k^{(1b)}\rangle = \sum_l (\boldsymbol{r}' - \boldsymbol{d}_k) \times G_{kl} \boldsymbol{p} |\phi_l^{(0)}\rangle \cdot \boldsymbol{B}, \tag{12}$$

$$|\phi_k^{(1c)}\rangle = \sum_l G_{kl}(\boldsymbol{d}_k - \boldsymbol{d}_l) \times \boldsymbol{p} |\phi_l^{(0)}\rangle \cdot \boldsymbol{B}. \tag{13}$$

Here, G_{kl} denotes the Green's function and $\boldsymbol{d}_k$ is the center of charge of the corresponding MLW orbital. The Green's function is given by

$$G_{kl} = \sum_{o,u} U_{ko}^\dagger \frac{|\phi_u\rangle\langle\phi_u|}{\epsilon_o - \epsilon_u} U_{ol}, \tag{14}$$

where ϵ_o and ϵ_u represent the Kohn-Sham energies of the occupied and unoccupied orbitals, respectively.

Within the CSGT method, the magnetic response is invariant under a translation of the coordinate system for every individual orbital. This allows us to redefine the position operator, thereby exploiting the spatial localization of the MLW orbitals. A sawtooth-shaped position operator is constructed for every orbital featuring the same periodicity as the simulation cell, with its geometric center located at the center of charge of the corresponding orbital. In doing so, the position operator has the required periodicity of the system, although it shows unphysical behavior around the borders. This, however, does not pose a significant problem as these unphysical transitions of the position operator occur in those regions of space where the state on which it is operating vanishes anyway. It is important to note that for a system with completely delocalized orbitals, like a metal, the decay of the MLW orbitals is insufficient, and therefore this approach will likely fail, unless prodigious simulation cell dimensions are adopted. In that case, the MPL method will be more efficient.

The actual calculation of the first-order corrections to the KS orbitals in the magnetic field is not performed using Green's functions. Instead, they are computed by minimization of the energy functional of second order in the magnetic field, for which a variational principle applies,[19] yielding these first-order corrections.

The full evaluation of Eqs. (11) and (12) for all electronic states k at once can be performed at the computational cost of approximately one total energy calculation. On the other hand, the computation of Eq. (13), which often represents a fairly small correction as compared to Eqs. (11) and (12), is much more intensive as it requires one calculation for every electronic state k (although typically at a lower computational cost than one total energy calculation[20,21]). This aspect hinders the practical use of the Sebastiani method. However, we do not always need to evaluate Eq. (13) for every electronic state k, as we will argue in the following. Since the SO [Eq. (6)] term is found to dominate the SOO [Eq. (7)] term by far in most cases, we focus our attention on the former.

The integrandum of $\Delta g_{xy}^{\mathrm{SO}}$ is composed of a substraction of spin α and spin β contributions. Assuming only small differences between the two effective potentials $V_{\mathrm{eff}}^{\alpha}(\boldsymbol{r})$ and $V_{\mathrm{eff}}^{\beta}(\boldsymbol{r})$, it is superfluous to calculate the corrections of Eq. (13) to $\boldsymbol{j}_{B_x}^{\tau}(\boldsymbol{r})$ for pairs of α and β states that remain unaffected by the presence of the unpaired electron (and thus resemble each other), because they are canceled out anyway. This is especially the case for paramagnetic defects embedded in a crystalline environment, for which this theory is intended. In that case the unpaired electron is often localized in one part of the supercell and will affect merely its near vicinity. Other parts of the periodic box such as the lattice environment at a larger distance of the defect will be less affected.

The overlap with the unpaired electron could be used as an indicator that an evaluation of Eq. (13) may be needed for a particular state. However, due to the Wannier localization, the wave function of the unpaired electron is no longer directly available, because it has been mixed up with other states during the unitary transformation. We therefore introduced the root norm of the spin density as an alternative indicator, as follows:

$$\alpha_k = \int d\boldsymbol{r} \sqrt{|\rho_{\mathrm{spin}}(\boldsymbol{r})|} \cdot |\phi_k(\boldsymbol{r})|. \tag{15}$$

Only if an expansion coefficient α_k exceeds a certain threshold is the calculation of $|\phi_k^{(1c)}\rangle$ performed. This approximation allows for a drastic reduction in computation time in the study of paramagnetic defects in a crystalline environment, without compromising the accuracy of the calculations. This reduction is applicable only in the case of g tensor calculations and not, for example, in the case of NMR chemical shielding tensor calculations, where Eq. (13) had to be neglected in order to make the method computationally efficient.

C. Implications of the pseudopotential approach

The method as described here was implemented in the CPMD program package,[22] a frequently used molecular dynamics code based on a plane-wave pseudopotential implementation, resulting in the absence of core electrons as well as in an inaccurate description of the valence orbitals in a spherical region around the core of each element defined during construction of the pseudopotential, hereafter referred to as the core region.

While this method has proven successful in describing chemical bonding, no evidence is available that the use of pseudopotentials could produce equally meaningful results for the EPR g tensor. However, since the g tensor is essentially a valence property[10,23] and depends less critically on the exact behavior of the electronic wave functions near the cores (as compared to the NMR shielding tensor, for which a pseudopotential approach does in fact work[9]), we believed that the g tensor would not suffer too much from the incorrect shape of the orbitals in the core regions.

By careful analysis of Eqs. (5)–(7), we will now argue that most of the errors introduced by the pseudopotentials can be traced back to the incorrect shape of the unpaired electron in the core regions.

(i) In the $\Delta g_{xy}^{\mathrm{ZKE}}$ term, spin α and β kinetic energies are substracted from each other. The shape of the orbitals in the core regions is largely determined by the strong attractive nuclear potentials. For this reason, the faulty contributions within the core regions in the kinetic energies from paired electrons will cancel out. Thus, the main erroneous contribution comes from the kinetic energy part of the unpaired electron in the core regions. The $\Delta g_{xy}^{\mathrm{ZKE}}$ term is isotropic, and these errors will therefore not influence the direction of the principal axes.

(ii) The same considerations apply to the $\Delta g_{xy}^{\mathrm{SO}}$ term, in which the erroneous contributions in the core regions from paired electrons cancel each other out: due to the dominant nuclear potentials, both effective potentials (and hence their gradients) and the current densities from the paired electrons will resemble each other in the core regions. Thus, the major errors originate from the cross product of the current of the unpaired electron and the gradient of the effective potential in the core regions: $[j_{\boldsymbol{B}_x}^{\alpha}(\boldsymbol{r}) - j_{\boldsymbol{B}_x}^{\beta}(\boldsymbol{r})] \times \nabla V_{\mathrm{eff}}(\mathbf{r})$. Unfortunately, the gradient of the effective potential largely favors the current of the unpaired electron near the cores. In addition, the

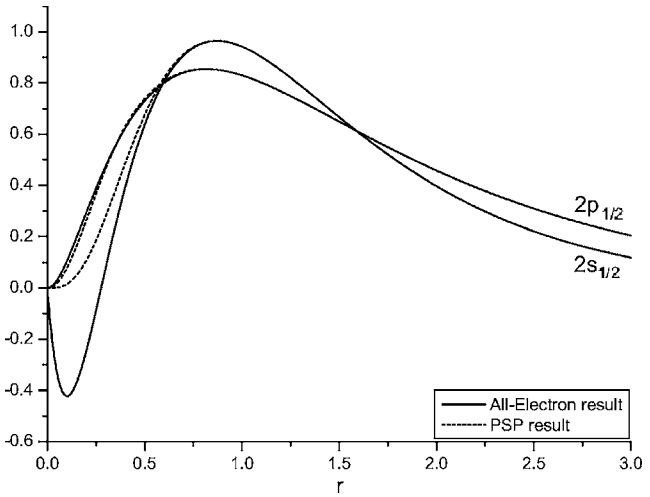

FIG. 1. $2s_{1/2}$ and $2p_{1/2}$ pseudo and all-electron wave functions of the free O atom.

$\Delta g_{xy}^{\mathrm{SO}}$ term is found to be by far the most dominant contribution to the total g tensor.

(iii) In the $\Delta g_{xy}^{\mathrm{SOO}}$ term, the pseudopotential approximation is expected to result in only small errors to the total Δg tensor, because the $\Delta g_{xy}^{\mathrm{SOO}}$ term is found to be very small in comparison with the $\Delta g_{xy}^{\mathrm{SO}}$ term,[5] and because both the induced magnetic field and the spin density do not diverge near the cores.

From this discussion we can conclude that, since $\Delta g_{xy}^{\mathrm{SO}}$ is generally the most important term, a good description of the current of the unpaired electron is the most essential precondition for the success of our pseudopotential method. There are some arguments why this will be the case even when using pseudopotentials. At least for the free atom, the more energetic orbitals do not suffer to the same extent from the use of pseudopotentials in the core region. This is illustrated in Fig. 1 for the $2s_{1/2}$ and $2p_{1/2}$ orbitals of the free O atom. While the $2s_{1/2}$ wave functions completely deviate in the core region, the $2p_{1/2}$ pseudo-wave-function still closely resembles its all-electron counterpart. Close to the core, where a wave function is essentially atomlike (because of the dominating nuclear potential), the unpaired electron wave function will mainly be composed of these more energetic atomic orbitals. In addition, the construction of a pseudopotential for a specific atomic element is not unique. An important degree of freedom is the size of the core region (while acknowledging that the smaller the core region, the higher the computational cost).

III. RESULTS

To validate our pseudopotential approach for the evaluation of the g tensor, we made a comparative study with the all-electron Schreckenbach and Ziegler (SZ) method as well as with experimental data from the literature for a series of small isolated molecules. We also included results from the ZORA approach of Van Lenthe *et al.*,[24] which is based upon a different theoretical approach. We approximated the isolated molecules in the CPMD program package by using large supercells of $(20\ \mathrm{a.u.})^3$. After Wannier localization, we can assume the Wannier orbitals to be so well confined within the supercell that any errors due to the aforementioned nonphysical behavior of the coordinate operator are excluded. The results given are a measure for the accuracy one can expect from a pseudopotential approach without reconstruction techniques for the valence orbitals in the core region. Troullier-Martins[25] (TM) and Goedecker[15] (GO) norm-conserving pseudopotentials were used in this work. Plane-wave cutoff values of 100 Ry (TM) and 150 (GO) were found to yield more than reasonable convergence. These are approximately 30 Ry higher than typically used to describe chemical bonding. Optimized geometries were obtained with the ADF[26–28] package and used throughout. We used PBE[29] gradient corrected functionals in all calculations, and a QZ4P basis set for the nonperiodic calculations. We have also performed the calculations using a BLYP[30,31] functional, but the results have not been reported here, since the choice of the functional only marginally alters the results and does not reveal any additional relevant aspects.

In Table I, the results for radicals composed of lighter elements up to Ne are presented. For both types of pseudopotentials, there is a striking resemblance between our results and those obtained using the SZ method. This accordance could be expected, as both methods are closely related with each other. The deviations that are present should be attributed almost entirely to the effects of pseudopotentials. More insight can be gained from the statistical parameters (see Table II) deduced from the three methods using the data of Table I, whenever experimental results were available. In this statistical study, the predictions of Δg_{zz} for the molecules O_2H and H_2O^+ have been omitted as they perturb completely the statistical parameters for all methods. From Table II, the good agreement between our results and the SZ results becomes particularly clear: the correlation coefficient, the correlation slope, and the standard deviation all agree to within 5% (even within 1% for the GO results), while the SZ method, the ZORA method, and the experimental results deviate on a much larger scale. The good agreement is further confirmed in Table III, where we compare the different contributions to the g tensor for the O_3^- molecule. Summarizing, we believe that it is fair to state that our pseudopotential approach performs equally well as the SZ method in predicting Δg values for lighter elements.

Less accurate results were obtained when studying radicals with heavier elements than Ne, as can be observed from Table IV. Here, the effects of the use of pseudopotentials clearly become apparent, and the available results in Table IV from Ref. 5 show the superior behavior of the GIPAW method for these elements. In many cases, however, the calculated numbers from our method still exhibit at least the right trend. In order to produce better results for these heavier elements, a smaller core region is required. This can be accomplished by including more electrons explicitly in the calculations than required to adequately describe chemical bonding. This will result in a much better description of the electronic wave functions near the core, and as a result, a reduced core region.

To illustrate this, we have plotted the $3s_{1/2}$ and the $3p_{1/2}$ wave functions for the free Si atom in Fig. 2, using the stan-

TABLE I. Calculated Δg values (in ppm) for a series of small isolated molecules composed of elements up to Ne, using the standard Troullier-Martins and Goedecker pseudopotential sets supplied with CPMD, in comparison with experiment and other treatments. For comparison with the SZ results, we omit in this table the SOO contribution to our calculations.

			This method[b]			
Molec.	g value	Expt.[a]	TM	GO	SZ[b,c]	ZORA[b,c]
H_2^+	$\Delta g_{\parallel}$		−31	−31	−40	−66
	$\Delta g_{\perp}$		−37	−37	−43	−68
O_2H	Δg_{xx}	−800	−265	−272	−301	−2401
	Δg_{yy}	5580	5692	5905	6322	5072
	Δg_{zz}	39720	28007	27479	30391	90273
H_2O^+	Δg_{xx}	200	−174	−138	−204	−801
	Δg_{yy}	4800	5013	5233	5106	7159
	Δg_{zz}	18800	13048	13489	14416	47268
CO_2^-	Δg_{xx}	−4800	−4814	−4674	−5537	−5312
	Δg_{yy}	−500	−986	−866	−798	−678
	Δg_{zz}	700	569	599	742	1153
O_3^-	Δg_{xx}	200	−503	−507	−512	−441
	Δg_{yy}	10000	8365	9244	10533	12565
	Δg_{zz}	16400	17543	18240	17927	23041
CH_3	$\Delta g_{\parallel}$		−105	−61	−89	−123
	$\Delta g_{\perp}$		622	931	821	1147
NH_3^+	$\Delta g_{\parallel}$		−138	−98	−149	−206
	$\Delta g_{\perp}$		1834	2385	2195	3190
HCO	Δg_{xx}	−7500	−10108	−10329	−9764	−12372
	Δg_{yy}	0	−136	−192	−263	−194
	Δg_{zz}	1500	2848	2739	2832	3285
H_2CO^+	Δg_{xx}	−800	−1307	−1300	−1408	−1899
	Δg_{yy}	200	145	122	61	−282
	Δg_{zz}	4600	6413	6519	6410	7510
BO	$\Delta g_{\parallel}$	−800	−70	−77	−71	−118
	$\Delta g_{\perp}$	−1100	−2975	−2753	−2335	−2487
C_3H_5	Δg_{xx}	0	−106	−91	−110	−118
	Δg_{yy}	400	528	872	704	887
	Δg_{zz}	800	561	926	832	1084
CO_3^-	$\Delta g_{\parallel}$	4300	4905	4848	3474	3330
	$\Delta g_{\perp}$	11200	10985	12234	11952	17237
NO_2	Δg_{xx}	−11300	−14204	−14901	−14048	−16419
	Δg_{yy}	−300	−1118	−1029	−768	−734
	Δg_{zz}	3900	2488	3084	4296	5044
CH_4^+	Δg_{xx}	600	−114	−74	−108	−144
	Δg_{yy}	600	556	862	739	988
	Δg_{zz}	600	556	862	739	988
NF_2	Δg_{xx}	−100	−704	−745	−688	−324
	Δg_{yy}	2800	2735	3493	4819	6532
	Δg_{zz}	6200	6908	7752	7836	10866
NF_3^+	$\Delta g_{\parallel}$	1000	−797	−834	−586	−195
	$\Delta g_{\perp}$	7000	4782	6011	8045	10356
CO^+	$\Delta g_{\parallel}$	−3200	−3960	−3918	−3194	−3543
	$\Delta g_{\perp}$	−1400	−80	−17	−136	−200
CN	$\Delta g_{\parallel}$	−800	−134	−94	−134	−184
	$\Delta g_{\perp}$	−2000	−2835	−3223	−2556	−2730
NO_3	$\Delta g_{\parallel}$	4300	1237	1033	167	−261
	$\Delta g_{\perp}$	13550	11202	12660	12261	16850

[a]Experimental values are quoted from Refs. 3 and 32. Most experimental measurements were performed in solid matrices, with the exception of O_2H, H_2O^+, NO_2, and NF_2.

[b]Using optimized geometries obtained with ADF (QZ4P basis set, PBE functional).

[c]The g tensor principal values in the SZ and ZORA method were computed in this work, using ADF (QZ4P basis set, PBE functional).

dard Goedecker pseudopotential provided with the CPMD package with $3s^23p^2$ as valence states and a modified Goedecker pseudopotential with $2s^22p^63s^23p^2$ as valence states, and compared it with the all-electron result. The modified pseudopotential manifestly better reproduces the correct oscillating behavior of the all-electron wave functions in the core region, and hence will produce better results for the g tensor. In order to describe these extra nodes correctly, a higher number of plane waves is needed in the basis set, which can be computationally demanding. However, in many cases this harder but more accurate pseudopotential will yield better results at even moderate cutoff energies. We have verified the previous statements for MgF, AlO, and SiH_3 in Table V. We found that an increase of the number of valence electrons results in a better agreement already at 150 Ry, although a higher cutoff was needed to yield fully converged results. In the study of paramagnetic defects embedded in a crystalline environment, we therefore recommend using a modified hard pseudopotential for the heavier atoms of the defect, even at a lower plane-wave energy cutoff.

TABLE II. Statistics of the calculated Δg values (in ppm) in the various methods. All values are taken from Table I, whenever experimental results are available. The linear regression parameters were obtained from a plot of the calculated versus the experimental Δg values.

	This method			
	TM	GO	SZ	ZORA
Correlation coefficient	0.977	0.981	0.980	0.972
Correlation slope	1.034	1.102	1.094	1.365
Standard deviation	1170	1241	1228	2529
Maximum deviation	−3063	−3601	−4133	6641
Mean unsigned error	901	929	890	1804
Mean signed error	−435	−221	−94	528

TABLE III. Deviation from the SZ result of the different contributions to the g values of O_3^-, using Goedecker pseudopotentials.

		abs. error (ppm)	pct. error (%)
Δg^{ZKE}		8	2.2
Δg^{SO}			
	Δg_{xx}^{SO}	3	1.6
	Δg_{yy}^{SO}	1297	11.9
	Δg_{zz}^{SO}	305	1.7

TABLE IV. Calculated Δg values (in ppm) for a series of small isolated molecules with heavier elements than Ne, using the standard Goedecker pseudopotential sets supplied with CPMD, in comparison with experiment and other treatments. For comparison with the SZ results, we omit in this table the SOO contribution to our calculations.

			This method[b]			
Molec.	g value	Expt.[a]	GO	SZ[b,c]	ZORA[b,c]	GIPAW[d]
MgF	$\Delta g_{\parallel}$	−300	−7	−59	−81	−49
	$\Delta g_{\perp}$	−1300	−1091	−2156	−1968	−2093
SO_3^-	$\Delta g_{\parallel}$		−450	−43	162	
	$\Delta g_{\perp}$		1315	2008	2746	
SO_2^-	Δg_{xx}	−400	−220	−352	−531	
	Δg_{yy}	3400	3796	4881	4901	
	Δg_{zz}	9700	4565	4999	5030	
ClO_3	$\Delta g_{\parallel}$	5000	801	1133	2091	
	$\Delta g_{\perp}$	6000	4908	5680	6707	
ClO_2	Δg_{xx}	1300	−241	−487	−666	
	Δg_{yy}	6500	7107	11481	12458	
	Δg_{zz}	16000	9887	13193	15637	
AlO	$\Delta g_{\parallel}$	−900	−59	−137	−364	−141
	$\Delta g_{\perp}$	−2600	3543	−2192	1128	−2310
BS	$\Delta g_{\parallel}$	−700	−21	−81	−471	−80
	$\Delta g_{\perp}$	−8100	−976	−10123	12276	−9901
KrF	$\Delta g_{\parallel}$	−2000	−185	−337	−16603	−340
	$\Delta g_{\perp}$	66000	30916	61668	26471	61676
XeF	$\Delta g_{\parallel}$	−28000	−173	−334	−67027	−333
	$\Delta g_{\perp}$	124000	19128	157380	94719	151518
SiH_3	$\Delta g_{\parallel}$	1000	2	−111	−151	
	$\Delta g_{\perp}$	5000	128	2570	3779	
GeH_3	$\Delta g_{\parallel}$	1000	−19	−65	−1675	
	$\Delta g_{\perp}$	15000	67	18591	24104	
SnH_3	$\Delta g_{\parallel}$	1000	−21	−248	−11219	
	$\Delta g_{\perp}$	23000	14	36929	47031	

[a]Experimental values are quoted from Ref. 3. All experimental measurements were performed in solid matrices.

[b]Using optimized geometries obtained with ADF (QZ4P basis set, PBE functional).

[c]The g tensor principal values in the SZ and ZORA method were computed in this work, using ADF (QZ4P basis set, PBE functional).

[d]Results from Pickard and Mauri (Ref. 5).

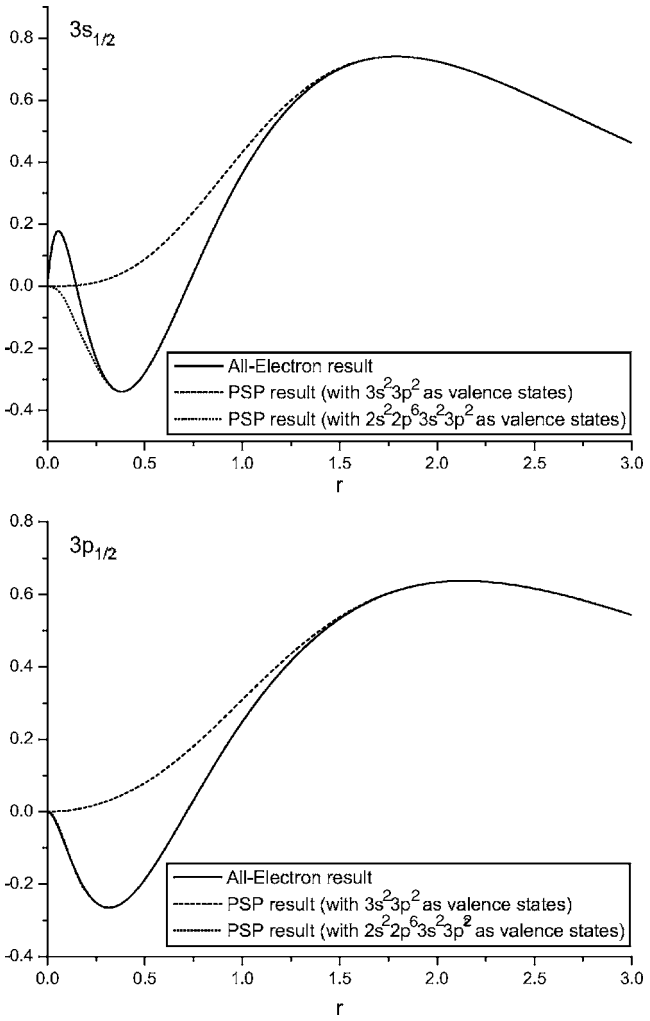

FIG. 2. $3s_{1/2}$ (upper graph) and $3p_{1/2}$ (lower graph) orbitals of the free Si atom using a soft and a hard Goedecker pseudopotential. Note that the hard pseudopotential (PSP) $3p_{1/2}$ orbital corresponds entirely with its all-electron counterpart.

The real application field of the method undoubtedly lies in the prediction of EPR parameters of paramagnetic defects in a crystal environment. Therefore, we further validated our approach by studying the O_3^- radical in a KCl lattice, in which as a function of the tilting angle α with $\langle 110 \rangle$ in the $\{1\bar{1}0\}$ plane, a metastable configuration at $\alpha=0°$ (untilted) and a stable configuration at $\alpha=34°$ (tilted) have been found theoretically,[34] as illustrated in Fig. 3. We modeled the latter with a 66-atom (31 Cl, 32 K, and 3 O) neutrally charged cubic cell, using a Goedecker pseudopotential, a BLYP functional, and a 80 Ry plane-wave cutoff, which is about the lower limit for this type of pseudopotential to obtain good results. In Table VI, the g values, as well as their principal directions, and the hyperfine values (using a method due to Van de Walle and Blöch,[35] which we also implemented in CPMD), are shown. Except for the incorrect prediction of the g_{xx} shift, from which all theoretical methods seem to suffer (see the O_3^- molecule in Table I and Ref. 36), a good agreement with available experimental g values is found, within the error margins of around 1000 ppm as argued by Neese in

TABLE V. Calculated Δg values (in ppm) for some selected molecules from Table IV, using harder pseudopotentials for the heavier elements Mg, Al, and Si. For comparison with the SZ results, we omit in this table the SOO contribution to our calculations.

		This method			
Molec.	g value	150 Ry[a]	150 Ry[b]	200 Ry[b]	SZ
MgF	$\Delta g_\perp$	−1091	−1734	−1813	−2156
	$\Delta g_\parallel$	−7	−17	−17	−59
AlO	$\Delta g_\parallel$	−59	−101	−100	−137
	$\Delta g_\perp$	3543	−634	−1942	−2192
SiH_3	$\Delta g_\parallel$	2	−61	−68	−111
	$\Delta g_\perp$	128	2125	2656	2570

[a]Using standard Goedecker pseudopotentials supplied with CPMD. The following states were explicitly used in the calculations: $3s^2$ for Mg; $3s^23p^1$ for Al; $3s^23p^2$ for Si.

[b]Using modified Goedecker pseudopotentials. The following states were explicitly used in the calculations: $2s^22p^63s^2$ for Mg; $2s^22p^63s^23p^1$ for Al; $2s^22p^63s^23p^2$ for Si.

Ref. 36. The directions of the principal axes are equally well predicted: the theoretical directions do not deviate from experiment by more than 0.7 degrees, and often only 0.2 degrees.

One of the goals of this paper is to present an efficient method for the calculation of the g tensor in extended periodic systems at a reasonable computational cost. In this context, we proposed a selection criterion to pick out those electronic states for which a calculation of the computational expensive $|\phi_k^{(1c)}\rangle$ term [Eq. (13)] is needed to get the required accuracy. Obviously, the lower the threshold value α_{thres}, the more attractive the method becomes due to the reduction of the computational effort. The determination of this threshold value should be submitted to a careful investigation to guarantee sufficient convergence, but the proposed selection criterion turns out to be very efficient, as will be shown now. In Fig. 4, we plot the correlation of the theoretical predictions of Δg with respect to the experiment for the O_3^- radical in a KCl lattice. We considered the two extreme cases (full calculation of $|\phi_k^{(1c)}\rangle$ versus complete neglect of this term) and

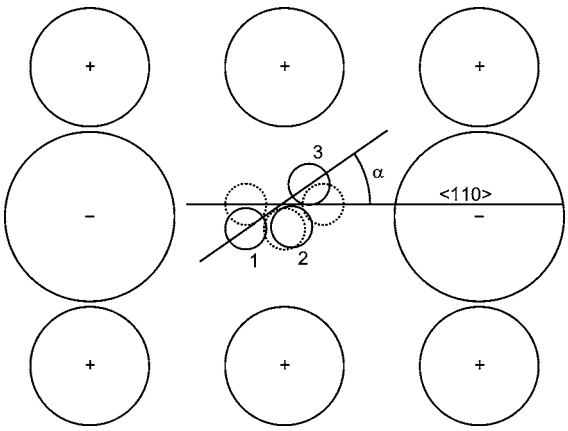

FIG. 3. $\{1\bar{1}0\}$-plane: Configuration of O_3^- in KCl.

TABLE VI. Calculated EPR values (Δg values in ppm, hyperfine values in Mhz) for O_3^- in KCl in the tilted configuration ($\alpha = 34°$).

g tensor			Expt.[33]	This method
Δg_{xx}			681	−452
Δg_{yy}			15981	16839
Δg_{zz}			9381	9434
$\alpha = \angle(g_{yy})$ with $\langle 110\rangle$			35°	34.8°
$\angle(g_{yy})$ with $\{1\bar{1}0\}$			0°	0.2°
$\angle(g_{xx})$ with $\langle 1\bar{1}0\rangle$			0°	0.1°
$\angle(g_{xx})$ with $\{001\}$			0°	0.2°
$\angle(g_{zz})$ with $\langle 001\rangle$			35°	34.8°
$\angle(g_{zz})$ with $\{1\bar{1}0\}$			0°	0.7°
Hyperfine tensor	A_{iso}	$A_{\text{ani},xx}$	$A_{\text{ani},yy}$	$A_{\text{ani},zz}$
O_1	−69.61	54.34	53.58	−107.92
O_2	−108.65	71.24	74.56	−145.81
O_3	−68.95	54.17	53.39	−107.57

the intermediate case completely determined by the chosen threshold value α_{thres} (in the figure a value of 0.01 was used). The numerical results of Fig. 4 obviously stress the importance of taking into account the contributions of the $|\phi_k^{(1c)}\rangle$ term, but a full calculation is far from being a prerequisite as the threshold algorithm manifestly predicts the same values. The computational effort of the threshold calculation was only little more than needed for the calculation in which $|\phi_k^{(1c)}\rangle$ was completely neglected.

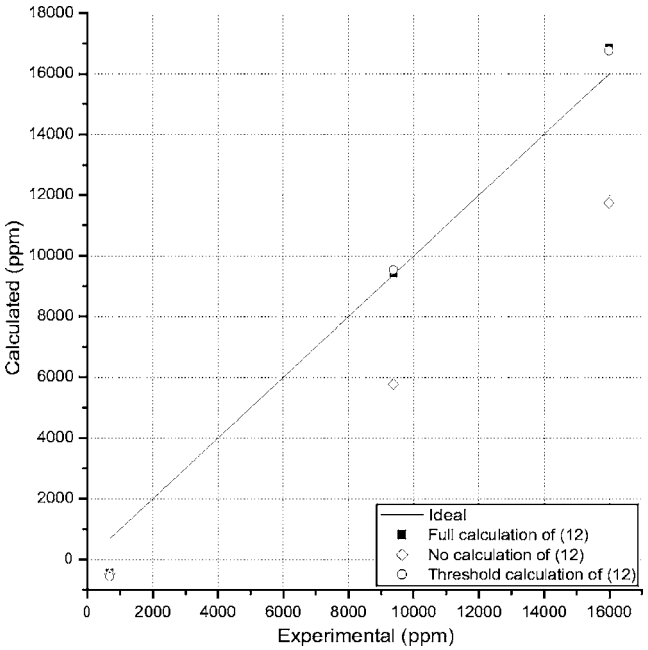

FIG. 4. Calculated Δg values for O_3^- in KCl in the tilted configuration. Comparison of the different methods for the calculation of Eq. (13). $\alpha_{\text{thres}} = 0.01$ was used in the threshold calculation.

IV. CONCLUSION

We have developed an alternative method for the calculation of the EPR *g* tensor in extended periodic systems, based on a pseudopotential approach without reconstruction techniques and the Sebastiani method. The method has been implemented in the CPMD code.

We have shown that for radicals composed of lighter elements (up to Ne) in the Periodic Table, the prediction of the *g* tensor is slightly suffering from the use of pseudopotentials, and accuracies similar to the all-electron Schreckenbach and Ziegler calculations were obtained with different types of norm-conserving pseudopotentials. For radicals with heavier elements than Ne, more electrons than strictly required to describe chemical bonding need to be included in the calculation.

The method comes at an attractive computational cost.

Together with the molecular dynamics capabilities of the CPMD package, we plan to use our method for EPR studies at finite temperatures. Calculations on relevant applications are in progress and look promising. We expect the extension of the CPMD code to be of great value in *ab initio* predictions of the EPR *g* tensor.

ACKNOWLEDGMENTS

This work is supported by the Fund for Scientific Research–Flanders and the Research Board of Ghent University. The authors wish to express their gratitude to J. Hutter, D. Sebastiani, and F. Mauri for discussions and kind support.

*Electronic address: Michel.Waroquier@UGent.be

[1] P. Hohenberg and W. Kohn, Phys. Rev. **136**, B864 (1964).
[2] W. Kohn and L. Sham, Phys. Rev. **140**, A1133 (1965).
[3] G. Schreckenbach and T. Ziegler, J. Phys. Chem. A **101**, 3388 (1997).
[4] M. Kaupp, M. Bühl, and V. G. Malkin, *Calculations of NMR and EPR Parameters: Theory and Applications* (Wiley-VCH, Weinheim, 2004).
[5] C. J. Pickard and F. Mauri, Phys. Rev. Lett. **88**, 086403 (2002).
[6] C. J. Pickard and F. Mauri, Phys. Rev. B **63**, 245101 (2001).
[7] P. E. Blöchl, Phys. Rev. B **50**, 17953 (1994).
[8] F. Mauri, B. G. Pfrommer, and S. G. Louie, Phys. Rev. Lett. **77**, 5300 (1996).
[9] D. Sebastiani and M. Parrinello, J. Phys. Chem. A **105**, 1951 (2001).
[10] G. Schreckenbach, Ph.D. thesis, University of Calgary, Calgary (1996).
[11] S. Patchkovskii and T. Ziegler, J. Phys. Chem. A **105**, 5490 (2001).
[12] J. E. Harriman, *Theoretical Foundations of Electron Spin Resonance* (Academic Press, New York, 1978).
[13] E. van Lenthe, P. E. S. Wormer, and A. van der Avoird, J. Chem. Phys. **107**, 2488 (1997).
[14] O. L. Malkina, J. Vaara, and B. Schimmelpfennig, J. Am. Chem. Soc. **122**, 9206 (2000).
[15] S. Goedecker, M. Teter, and J. Hutter, Phys. Rev. B **54**, 1703 (1996).
[16] G. Wannier, Phys. Rev. **52**, 191 (1937).
[17] W. Kohn, Phys. Rev. **115**, 809 (1959).
[18] T. Keith and R. Bader, Chem. Phys. Lett. **210**, 223 (1993).
[19] A. Putrino, D. Sebastiani, and M. Parrinello, J. Chem. Phys. **113**, 7102 (2000).
[20] D. Sebastiani, G. Goward, I. Schnell, and M. Parrinello, Comput. Phys. Commun. **147**, 707 (2002).
[21] D. Sebastiani, G. Goward, I. Schnell, and H. W. Spiess, J. Mol. Struct. **625**, 283 (2003).
[22] Car-Parrinello Molecular Dynamics, version 3.9.2; Copyright IBM Corp., 1990–2005.
[23] M. Kaupp, *EPR Spectroscopy of Free Radicals in Solids. Trends in Methods and Applications*, edited by A. Lund and M. Shiotani (Kluwer, Dordrecht, 2003).
[24] E. Van Lenthe, A. van der Avoird, W. R. Hagen, and E. J. Reijerse, J. Phys. Chem. A **104**, 2070 (2000).
[25] N. Troullier and J. L. Martins, Phys. Rev. B **43**, 1993 (1991).
[26] G. te Velde, F. M. Bickelhaupt, S. J. A. van Gisbergen, C. Fonseca Guerra, E. J. Baerends, J. G. Snijders, and T. Ziegler, J. Comput. Chem. **22**, 931 (2001).
[27] C. Fonseca Guerra, J. G. Snijders, G. te Velde, and E. J. Baerends, Theor. Chem. Acc. **99**, 391 (1998).
[28] ADF2004.01, SCM, Theoretical Chemistry, Vrije Universiteit, Amsterdam, The Netherlands, http://www.scm.com.
[29] J. P. Perdew, K. Burke, and M. Ernzerhof, Phys. Rev. Lett. **77**, 3865 (1996).
[30] A. D. Becke, Phys. Rev. A **38**, 3098 (1988).
[31] C. Lee, W. Yang, and R. G. Parr, Phys. Rev. B **37**, 785 (1988).
[32] D. Jayatilaka, J. Chem. Phys. **108**, 7587 (1998).
[33] F. Callens, P. Matthys, and E. Boesman, J. Phys. C **21**, 3159 (1988).
[34] V. Van Speybroeck, E. Pauwels, F. Stevens, F. Callens, and M. Waroquier, Int. J. Quantum Chem. **101**, 761 (2005).
[35] C. G. Van de Walle and P. E. Blöchl, Phys. Rev. B **47**, 4244 (1993).
[36] F. Neese, J. Chem. Phys. **115**, 11080 (2001).